ORIGINAL RESEARCH

Effect of Food-Grade Pharmaceutical Excipients on Physicochemical Behaviour of Quercetin Nanocomposites: Thermal and Non-Thermal Analysis

Article history:
Received: 22-12-2023
Revised: 09-04-2024
Accepted: 11-05-2024
Published: 18-10-2024

Sabya Sachi Das[a], Priya Ranjan Prasad Verma[b], Sandeep Kumar Singh[c]

Abstract: In this study, the compatibility of Quercetin (QC) nanocomposites with some selective food-grade pharmaceutical excipients was assessed using various thermal (DSC and TGA), non-thermal (P-XRD, FT-IR, and RAMAN spectroscopy, and FESEM) techniques. All techniques were simultaneously used and correlated to detect the QC's compatibility with the selected excipients (CO, CCO, OA, T20, T60, and T80). DSC-TG studies showed that QC-CO and QC-T60 samples exhibited irregular degradation patterns, causing the drug's transformation from crystalline to amorphous. P-XRD results showed that the crystalline behavior of QC was retained in all the samples. However, the peak intensities were reduced and shifted in some samples. The $D_{avg.}$ value for all samples, including pure QC, was 26.80-76.07 nm. FT-IR and RAMAN studies demonstrated that bonds including –C=O stretching, C-C stretching (ring A), and -OH bonds (in ring A, B, and C) in pure QC play a crucial role in its interaction with excipients. Furthermore, the excipients' effect on QC's morphology using FESEM showed smoothening, fragmentation, and agglomeration of the drug. In conclusion, the possible drug-excipient incompatibility can be potentially determined with the help of these analytical methods. The physicochemical studies from this work may provide immense knowledge for the researchers and manufacturers involved in quercetin-based pharmaceutical and/or nutraceutical formulations.

Keywords: Analytical characterizations; Drug-excipient Compatibility; Nanocomposites; Non-thermal studies; Quercetin; Thermal studies.

[a] School of Pharmaceutical and Population Health Informatics, DIT University, Dehradun, Uttarakhand, 248009, India. Corresponding author: ss.das@dituniversity.edu.in

[b] Department of Pharmaceutical Sciences and Technology, Birla Institute of Technology, Mesra, Ranchi, Jharkhand, 835215, India.

[c] Faculty of Science, School of Mathematical and Physical Sciences, University of Technology Sydney 15 Broadway, Ultimo NSW 2007, Australia. Corresponding author: dr.sandeep_pharmaceutics@yahoo.com

1. INTRODUCTION

Flavonoids are subtypes of natural polyphenols found as secondary metabolites in almost all parts of the plants. Among all flavonoids, Quercetin (QC; 3,3′,4′,5,7-pentahydroxyflavone) is abundantly found in various natural resources, including onion, green leafy vegetables, red wine, citrus fruits, cherries, raspberries, and others. QC (Fig. 1) is a potent naturally occurring antioxidant and has gained huge consideration by scientists and researchers worldwide to manage numerous diseases (D'Andrea, 2015; Das, Verma, Kar, Singh, 2020). The antioxidant properties of QC have been able to exhibit other therapeutic actions such as anticancer, antiviral, anti-infective, anti-inflammatory, antitumor, neurological disorders, and

anti-diabetic (Agrawal, Chakraborty, Dewanjee, Arfin, Das, Dey, Moustafa, Mishra, Jafari, Jha, Jha, Kumar, 2023; Das, Jha, Jha, Verma, Ashraf, Singh, 2023; Das, Sarkar, Chabattula, Verma, Nazir, Gupta, Ruokolainen, Kesari, Singh, 2022). In addition, QC also exhibits potential cell-protective activities in heart, liver, kidney, colon, and brain disorders or diseases (Bischoff, 2008; Das, Hussain, Verma, Imam, Altamimi, Alshehri, Singh, 2020; Das, Verma, Singh, 2020a). QC and its derivatives have exhibited various potential biological activities. However, it has been reported with two significant issues of low oral bioavailability (~16.2%) and poor aqueous solubility (0.17-7.7 mg/mL), so its clinical applications are restricted (Dinesh Kumar, Verma, Singh, 2015; Gao, Wang, Wei, Men, Zheng, Zhou, Zheng, Gou, Huang, Guo, Huang, Qian, Wei, 2012).

Additionally, QC is a photosensitive moiety and is also sensitive to oxidative degradation in the aqueous (alkaline pH) and organic phase, which causes instability of QC in the aqueous environment (Balestrin, Bidone, Bortolin, Moresco, Moreira, Teixeira, 2016; Liu, Hu, Lin, Chen, Zhu, Hou, Shi, 2013; Makris Rossiter, 2000). These limitations have exhibited impending effects in establishing efficient and stable QC formulations. Addressing and overcoming these limitations at the preformulation stage will ensure the robustness of product efficiency.

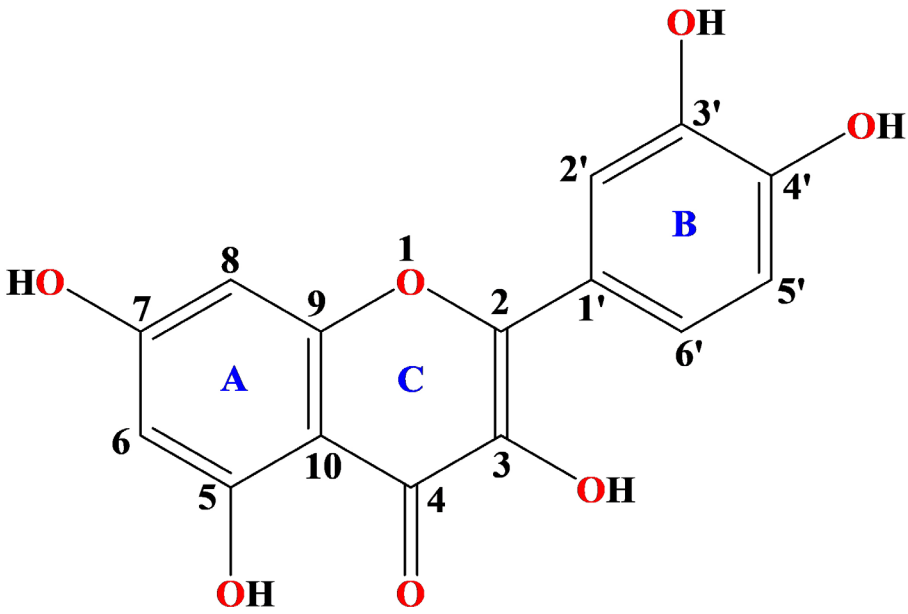

Figure 1. Molecular structure of Quercetin.

Various food-grade excipients such as lipids, oils, surfactants, co-surfactants, and others play a significant role and are used as major components by the pharmaceutical and food industries. The lipids and oils exhibit numerous desirable qualities such as color, odor, texture, arrangement, taste and others to the food products (German, 1999). Usually, the food quality is precisely associated with their lipid quality. The lipids present in the food products are essential elements of the cell structure and cellular membrane functions and have shown significant effects on our well-being. Moreover, the major cause for deprivation of food quality is related to the degradation and variation in the lipids/oils (Lillard, 1983). The emulsifying agents, surfactants or stabilizing agents have shown diverse functionality in the development or establishment of various food or food derivatives. Also, certain food-grade lipids have been reported to have potential anti-microbial activities and thus could be used in the food industries to detect the microbial load as well as to enhance the complete product quality (Singh, Hussain, Kumar Singh, 2020).

Apart from this, the oxidation of edible oils rich in PUFA (polyunsaturated fatty acids) is one of the most vital concerns of food industries as it directly impacts the flavor, nutrition, safety and storage issues (Kiokias, Gordon, Oreopoulou, 2017). It is very important to notice that various unsaturated lipids present in food or food by-products are highly

affected by lipid oxidation that causes reduced nutritional quality, shelf-life, and functionality. Usually, antioxidants, either natural or synthetic, are used to overcome this issue. The antioxidants either prolong the onset of oxidation or reduce the rate of lipid oxidation. Moreover, natural antioxidants (eg: quercetin-model antioxidant drug) can be used in place of synthetic antioxidants, due to their reported toxic effects, in food industries (Fuentes, Arias-Sante, Atala, Pastene, Kogan, Speisky, 2020; Garcia-Mendoza, Espinosa-Pardo, Savoire, Harscoat-Schiavo, Cansell, Subra-Paternault, 2021; Li S., Yan, Guan, Huang, 2020).

The preformulation studies provide essential information about the crucial parameters such as physicochemical stability, solubility, and permeability of the drugs and excipients used in formulations (Das, Verma, Singh, 2020b). In this context, drug-excipient interaction studies play a vital role in selecting excipients and establishing a stable formulation system. Moreover, interactions between the drug and excipient/s could cause significant modifications in the drug's stability and bioavailability. They thus could improve the therapeutic efficacy of the incorporated drug or bioactive (Das, Verma, Sekarbabu, Mohanty, Pattnaik, Ruokolainen, Kesari, Singh, 2023; Verma Garg, 2005). Olejniczak and Potrzebowski reported that QC exists both in the crystalline and anhydrous forms and stated that the hydration water molecules present in the QC molecule's crystal lattices highly influenced its molecular geometry (Olejniczak Potrzebowski, 2004). The physicochemical stability of the hydrophobic drugs highly depends upon the moisture temperature, pH, and other environmental factors. The process of hydration or dehydration may cause phase transitions (anhydrous to crystalline or vice-versa), instability and alterations in the physicochemical properties of hydrophobic drugs (Borghetti, Lula, Sinisterra, Bassani, 2009; Zhang, Law, Schmitt, Qiu, 2004).

Chemical interactions of excipients with the drug could degrade the drug's molecularity, whereas excipients' physical interactions with the drug could affect its solubility, dosing uniformity, and dissolution rate (Crowley Martini, 2001). The drug-excipient compatibility studies, being a part of pre-formulation studies, are very important for selecting excipients because they can interact both physically and chemically with the drug moiety and impact the stability of formulations (Bruni, Amici, Berbenni, Marini, Orlandi, 2002). Moreover, incompatibilities due to excipients such as oils/lipids and surfactants could affect the physicochemical properties, stability, and therapeutic efficacy of the drug and dosage form (Das, Verma, Singh, 2020b). Therefore, identifying probable incompatibilities between drug/s and various excipients at the preliminary phase helps develop and establish a stable formulation system or dosage forms (Thumma Repka, 2009).

Characterizing techniques such as differential scanning calorimetry (DSC), thermogravimetric analysis (TGA), powder X-ray powder diffraction (P-XRD), Fourier transform infrared (FT-IR) spectroscopy, Raman spectroscopy, and Field emission scanning electron microscopy (FESEM), are used for the drug-excipient compatibility studies (Bruni, Amici, Berbenni, Marini, Orlandi, 2002; Wyttenbach, Birringer, Alsenz, Kuentz, 2005). As per the reported literature, corn oil (Schoener, Zhang, Lv, Weiss, McClements, 2019), coconut oil (Alkhatib, Alyamani, Abdu, 2020), oleic acid (Barkat Ali, 2011; Gallelli, Cione, Serra, Leo, Citraro, Matricardi, Di Meo, Bisceglia, Caroleo, Basile, Gallelli, 2020), tween 20 (Anarjan Tan, 2013; Khalid, Kobayashi, Neves, Uemura, Nakajima, Nabetani, 2016), tween 60 (Anarjan Tan, 2013; Hemati, Haghiralsadat, Yazdian, Jafari, Moradi, Malekpour-Dehkordi, 2019), and tween 80 (Liu, Kobayashi, Russo, Li, Plevy, Gambling, Carson, Mumper, 2013; Sedaghat Doost, Kassozi, Grootaert, Claeys, Dewettinck, Van Camp, Van der Meeren, 2019) have exhibited significant role for the establishment of various drug delivery systems. Moreover, the various food-grade excipients used in this study, including corn oil (Dupont, White, Carpenter, Schaefer, Meydani, Elson, Woods, Gorbach, 1990), coconut oil (Seneviratne, HapuarachchI, Ekanayake, 2009), oleic acid (Sales-Campos, Reis de Souza, Crema Peghini, Santana da Silva, Ribeiro Cardoso, 2013), tween 20 (Teo, Goh, Wen, Oey, Ko, Kwak, Lee, 2016), tween 60 (Basiri, Rajabzadeh, Bostan, 2017) and tween 80 (Chassaing, Koren, Goodrich, Poole, Srinivasan, Ley, Gewirtz, 2015) have showed potential applications in food industries for the development and establishment of diverse food-products or by-products. Therefore, it becomes necessary for the researchers to monitor the significant effects of food-grade excipients over quercetin, a potential natural antioxidant, to establish stable and high-quality pharmaceutical, nutraceutical and cosmeceutical products. The physicochemical properties of these excipients have been summarized in Table 1.

Excipient Name	Chemical Composition	HLB Value	Major applications
Corn Oil	Palmittic acid, staeric acid, arachidic acid, oleic acid, α-linoleic acid, linoleic acid	NA*	• Used as oil base for the development of nano/micro-emulsions or self-emulsifying systems. • Used in the development of food products.
Coconut Oil	Caprylic acid, myristic acid, capric acid, lauric acid, palmitic acid, linoleic acid, stearic acid, oleic acid	NA*	• Used as an oil base for the development of nano/micro-emulsions or self-emulsifying systems. • Used in food and cosmetic product development.
Oleic Acid	Monounsaturated omega-9 fatty acid	1.6 (Barkat Ali, 2011)	• Antifoaming agent. • Used as an emulsifier or solubility enhancer.
Tween 20 (Polysorbate 20)	Polyoxyethylene sorbitan monolaurate	16.7 (Anarjan Tan, 2013)	• Non-ionic surfactant. • Emulsifying agent. • Used in formulating stable O/W emulsions. • Used as blocking agent for membrane-based immunoassays.
Tween 60 (Polysorbate 60)	Polyoxyethylene sorbitan monostearate	14.9 (Anarjan Tan, 2013)	• Non-ionic surfactant. • Emulsifying agent
Tween 80 (Polysorbate 80)	Polyoxyethylene sorbitan monooleate	15 (Liu, Kobayashi, Russo, Li, Plevy, Gambling, Carson, Mumper, 2013)	• Non-ionic surfactant. • Used as an emulsifying agent in the development of pharmaceutical, cosmeceutical and food products.

Table 1. Physico-chemical properties and major applications of excipients used in the compatibility studies. *(*NA: Not applicable).*

The present work aims to evaluate the significant effects of the selected excipients on Quercetin's nanocomposite physicochemical properties. Initially, the solubility studies were done to evaluate drug solubility in the selected excipients. The excess precipitates collected after solubility studies were then evaluated using thermal (DSC and TGA), non-thermal (P-XRD, FT-IR and Raman spectroscopy, and FESEM) methods as demonstrated in scheme 1.

2. EXPERIMENTATION

2.1. Materials

Quercetin (QC), corn oil (CO), oleic Acid (OA) and tween 60 (T60) were procured from Sigma Aldrich chemicals, USA. Tween 20 (T20) was procured from Loba Chemie Pvt. Ltd., India. Tween 80 (T80) was procured from Rankem, India. Coconut oil (CCO) was obtained from the local market. Water was collected from the Milli-Q water distillation system (Millipore, MA).

2.2. Methodology

2.2.1. Solubility studies

The solubility studies were accomplished through the shaking water bath method as reported in our previously reported work (Das, Verma, Singh, 2020b). As per the method, an excess amount of pure QC (~2 g) was added to the selected oils (CO, CCO and OA) and surfactants (T20, T60 and T80), and were placed in capped vials. Initially, vortexing of the capped vials was done for 5-15 min. Using a vortex mixture (REMI CM-101, India) for proper blending of the drug-excipient system and later

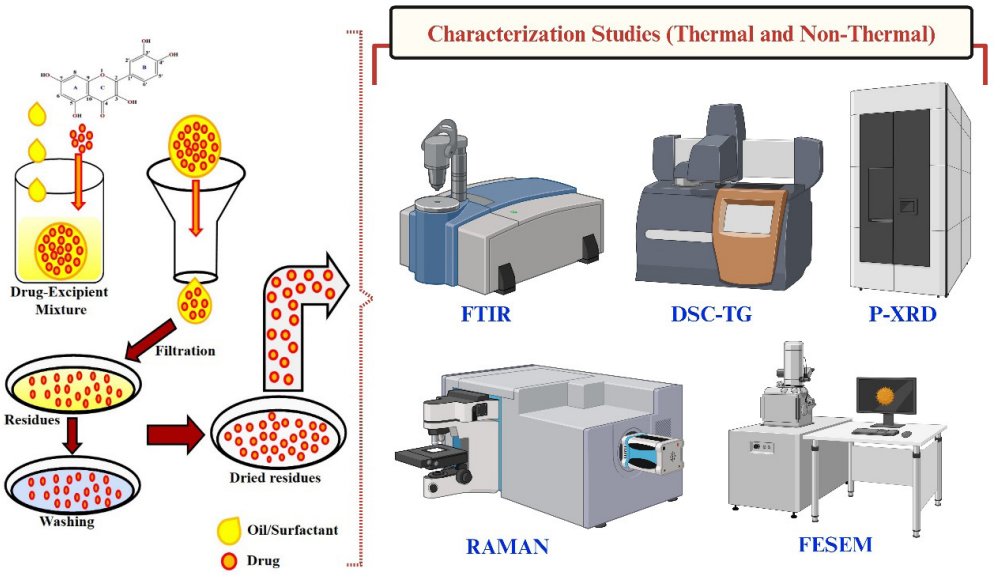

Scheme 1. Schematic representation of steps involved in the procurement of Group I: drug-oil residues (QC-CO, QC-CCO and QC-OA) and Group II: drug-surfactant residues (QC-T20, QC-T60 and QC-T80) and their evaluation using thermal (DSC and TGA), non-thermal (P-XRD, FT-IR and Raman spectroscopy, and FESEM) methods.

on, the vials were placed in a shaking water bath (REMI RSB-12, India) at 37 ± 3 °C. The shaking was maintained till saturation and after that, the dispersions were transferred into the Eppendorf tubes. Then the eppendorf tubes were vortexed, centrifuged (Eppendorf AG, Germany) at 11,000 g for 20 minutes and finally were filtered using a 0.45 µm membrane filter (Whatman, USA). Finally, the samples were analyzed with the help of an ultraviolet-visible spectrophotometer (UV-1800, Shimadzu, Japan). After solubility analysis, all the samples (drug-excipient nanocomposites residues) were categorized into two groups; Group I: drug-oil residues (QC-CO, and QC-OA) and Group II: drug-surfactant residues (QC-T20, QC-T60 and QC-T80), and further all the samples were intended for compatibility studies (Scheme 1).

2.2.2. Compatibility studies

The samples of group I and group II were rinsed with MilliQ water for complete removal of excipients and then centrifuged at 11,000g for 15 minutes. Later, all the samples were accumulated in sterilized and cleaned eppendorf tubes. These tubes were dehydrated and stored in the vacuum oven (NSW Pvt. Ltd., India), preserved at 45°C; 600 kPa, till further analysis. Moreover, the compatibility studies of Group I and Group II samples were performed using thermal (DSC and TGA) and non-thermal (P-XRD, FT-IR and RAMAN spectroscopy, and FESEM) methods.

2.2.2.1. Thermal analysis

Thermal analysis of all the samples, including pure QC, Group I and Group II residues were characterized using DSC and TG studies. Both the thermal analyses (DSC-TG) were accomplished using a simultaneous thermal analyzer (NETZSCH STA 449 F3 Jupiter, Germany). Initially, all the samples were weighed in a sterile DSC aluminum pan. Scanning of each sample was carried from ambient temperature to 500 °C with a 10 °C/min heating rate under an inert atmosphere (presence of nitrogen). The melting point (°C) and percent (%) mass loss of the samples were estimated from the DSC/TG curves using Proteus Software. Furthermore, to avoid any polymorphic alterations in the samples, neither of additional actions including compression, trituration and melting were implemented.

2.2.2.2. Non-thermal analysis

Non-thermal analysis of all the samples, including pure QC, Group I and Group II residues were characterized using P-XRD, FT-IR and Raman spectroscopy, and FESEM studies.

P-XRD studies of each sample were carried out at room temperature (25 ± 2 °C) by using Rigaku Smart Lab diffractometer system (Miniflex 600, Tokyo, Japan), having radiation (k) = 1.5406Å. Cu Kα was used as a source for the production of X-ray beams having emission current and system voltage of 35 mA and 40 kV, respectively. The samples were scanned within a range of 2θ = 5° to 50° at a scanning speed of 0.02°/sec (0.04° of step width and a count time of 60 sec.). The P-XRD patterns of each sample were refined and assessed using Smart Lab Guidance software. Furthermore, the mean particle size of the crystalline samples was estimated by calculating the FWHM and the Debye Scherrer's equation (equation 1),

$$D = \frac{K\lambda}{\beta \cos\theta} \quad \text{(Eq.1)}$$

Where, *D* is the mean crystallite size, *K* is Scherrer's constant (~0.94), λ is X-ray source wavelength (~0.154 nm), β is FWHM (full width at half maximum) of the most intense diffraction peak and θ is Bragg's diffraction angle (Kamoun, Gassoumi, Kouass, Alhalaili, Vidu, Turki-Kamoun, 2020; Ramachandran, Dash, Thamilselvan, Kalpana, Sundararajan, 2020; Tuncer, Bakan, Gocmez, Erdem, 2019).

FT-IR analysis of each sample was achieved using a Shimadzu 8400S FTIR spectrometer (Shimadzu, Japan). The spectra of each sample were noted in wavelength range of 4000-400 cm^{-1} having a spectral resolution of 4 cm^{-1} and with a scan count of 35. All the studies were performed at room temperature (25 ± 2 °C). Furthermore, IR Solutions software (version 1.21) was used for background deduction, baseline rectification, spectra normalization, spectra recordings and other significant calculations.

Raman spectral analysis of each sample was performed (3 scans) and recorded on Renishaw Raman *Invia* micro-Raman spectrophotometer at room temperature (25 ± 2 °C). Baseline correction and recording of Raman spectrum intensities (peak height) were done through WiRE software (version 3.3).

Morphological analysis of all the samples, including pure QC, Group I and Group II residues was done using FESEM (CARL ZEISS, Sigma 300, Germany) studies. The FESEM studies were performed at an accelerating voltage of 5 keV. Before analysis, each sample was mounted over the aluminum grid with the help of a double-sided adhesive tape, coated with gold and sputtered to make the grids charged and to achieve precise micrographs. The micrographs of each sample were acquired with a magnification range of 5.00 kX to 50.00 kX using FESEM control user interface (ZEISS SmartSEM Touch).

3. RESULTS AND DISCUSSIONS

3.1. Solubility studies

In our previously published work, we have reported the solubility of QC in some other excipients including Capmul MCM, Capmul MCM NF, Capryol PGMC, Cremophor RH40, Cremophor ELP and Transcutol HP. In this work, we have summarized the result of solubility studies of QC in selective oils and surfactants in Fig. 2. All the samples were performed in triplicates (n=3). It was observed that both Group I: drug-oil residues (QC-CO, QC-CCO and QC-OA) and Group II: drug-surfactant residues (QC-T20, QC-T60 and QC-T80) samples exhibited no major changes in their respective absorbance (studies through UV-Vis spectroscopy) when compared to pure QC. Furthermore, the solubility of QC in selective oils exhibited the pattern OA>CO>CCO and in selective surfactants followed the pattern T80>T60>T20.

As per the results availed from the solubility studies, QC showed maximum solubility in OA (oil) and T80 (surfactant) with the values of 4.24±0.68 and 76.30±1.90 mg/gm respectively. In previously reported works, it has been reported that although QC exhibits various pharmacological actions due to its solubility issues (poor aqueous soluble), its usage is restricted. Thus, these findings can assist researchers in exploring more QC by encapsulating into specific delivery systems including liposomes, emulsions, micelles, solid lipid nanoparticles and others (Das, Dubey, Verma, Singh, Singh, 2022; Kar S., Das, Kundu, Sahu, Kumar, Kesari, Singh, 2024; Kar Sweta, Das, Singh, 2023) to improve solubility leading to improved therapeutic effects.

3.2. Compatibility studies

3.2.1. Thermal Analysis

3.2.1.1. DSC-TG

DSC-TG thermograms of the pure QC, group I and group II samples are illustrated and detailed in Fig. 3. Further, Table 2 represents the summary of onset temperature (T_{onset}) and peak transition temperature (T_{peak}) for DSC curves of pure QC and

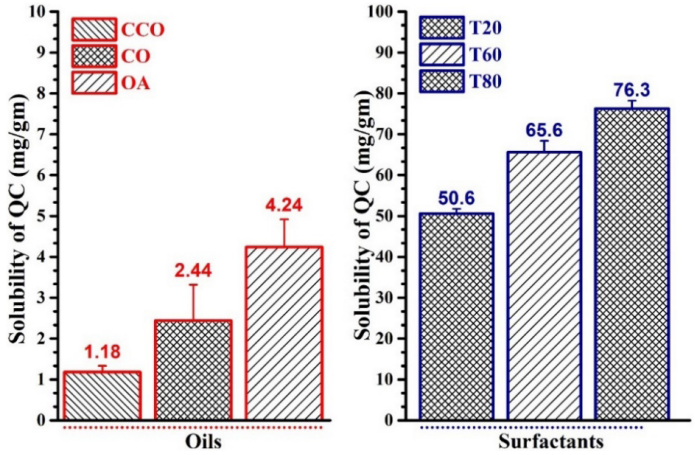

Figure 2. Solubility of quercetin (mg/gm) in excipients (oils and surfactants).Each sample was performed in triplicate (n=3).

various drug-excipient residues. Also, onset temperature (T_{onset}), endset temperature (T_{endset}) and percent mass loss (% mass loss) for TG curves of pure QC and various drug-excipient residues have been detailed in Table 2. DSC curve of pure QC (Fig. 3a) presented a broad and weak peak at 105.4 °C due to moisture loss. Furthermore, a sharp endothermic and a weak exothermic peak at 322.2 °C (degradation/melting point) and 348.4 °C (decomposition of the compound) respectively were observed, earlier reported in our work. TG curve showed the degradation events for pure QC within the range of 77.6-372.3 °C (~% mass loss of 27.7%). Moreover, similar findings were reported in the published literature (Manta, Papakyriakopoulou, Chountoulesi, Diamantis, Spaneas, Vakali, Naziris, Chatziathanasiadou, Andreadelis, Moschovou, Athanasiadou, Dallas, Rekkas, Demetzos, Colombo, Banella, Javornik, Plavec, Mavromoustakos, Tzakos, Valsami, 2020; Vaz, Clementino, Bidone, Villetti, Falkembach, Batista, Barros, Sonvico, Dora, 2020; Wang, Zou, Liu, Wang, Li, Shen, 2021).

The DSC curve of QC-CCO (Fig. 3c) and QC-OA (Fig. 3d) exhibited similar peak patterns as that of pure drugs. The TG curve showed degradation events for QC-CCO and QC-OA within the range 63.8-401.1°C (mass loss of~43%), and 89.4-381.6 °C (mass loss of~33%) respectively. The DSC curve of QC-CO (Fig. 3b) presented a thick moisture peak at 66.9 °C and multiple endothermic peaks at 281.8 °C, 302.9 °C and 376.1 °C which represented irregular degradation pattern of QC, possibly due to some chemical interaction with CO. The TG curve showed multiple degradation events for QC-CO within the range 38.4-404.5°C (mass loss of~57%). The DSC curve of QC-T20 (Fig. 3e) presented a peak at 70.4 °C (moisture loss) and a sharper endothermic peak at 294.1 °C. Also, an exothermic and an endothermic peak was noticed at 321.1°C and 335.9°C respectively. The DSC curve of QC-T60 (Fig. 3f) exhibited broad peaks fragmented at 30.7 °C and 52.6 (insignificant dehydration behavior). The curve exhibited two broad endothermic peaks (245.6 and 294.1 °C), and a weak endothermic peak (391.8 °C).

Compound	DSC Curves		TG Curves		Mass loss (%)
	T_{onset} (°C)	T_{peak}(°C)	T_{onset} (°C)	T_{endset} (°C)	
Pure QC	297.6	322.2	77.6	372.3	27.7
QC-CO	267.1; 286.5	281.8; 302.9	38.4	404.5	57.2
QC-CCO	298.1	321.9	63.8	401.1	43.5
QC-OA	301.3	322.6	89.4	381.6	33.3
QC-T20	273.1	294.1	46.6	376.6	38.9
QC-T60	211.4; 254.2	245.6; 263.4	5.5	403.4	72.2
QC-T80	268.7	292.9	26.6	359.5	36.7

Table 2. Thermoanalytical data of pure quercetin and quercetin-excipient nanocomposites residues.

Apart from this, an exothermic peak was observed at 328.7 °C. In this case, the degradation and decomposition patterns were inappropriate when compared to the thermograms of pure QC. The DSC curve of QC-T80 (Fig. 3g) exhibited broad peak at 82.7 (moisture loss) and a sharp endothermic peak at 292.9 °C (degradation) that was found to be shifted towards the left as compared to the DSC curve of pure QC (322.2 °C) Also, an exothermic peak was observed at 322.6 °C. The TG curve for QC-T20, QC-T60 and QC-T80 showed product decomposition within the range 46.6-376.6 °C (mass loss of ~ 38%), 5.5-403.4 °C (mass loss of ~72%) and 26.6-359.5 °C (mass loss of ~36%) respectively. The DSC/TG curves of QC-CO and QC-T60 samples, as compared to other samples, showed the degradation and decomposition of QC in irregular behavior, and thus the excipient might have changed the nature of the drug from crystalline to amorphous.

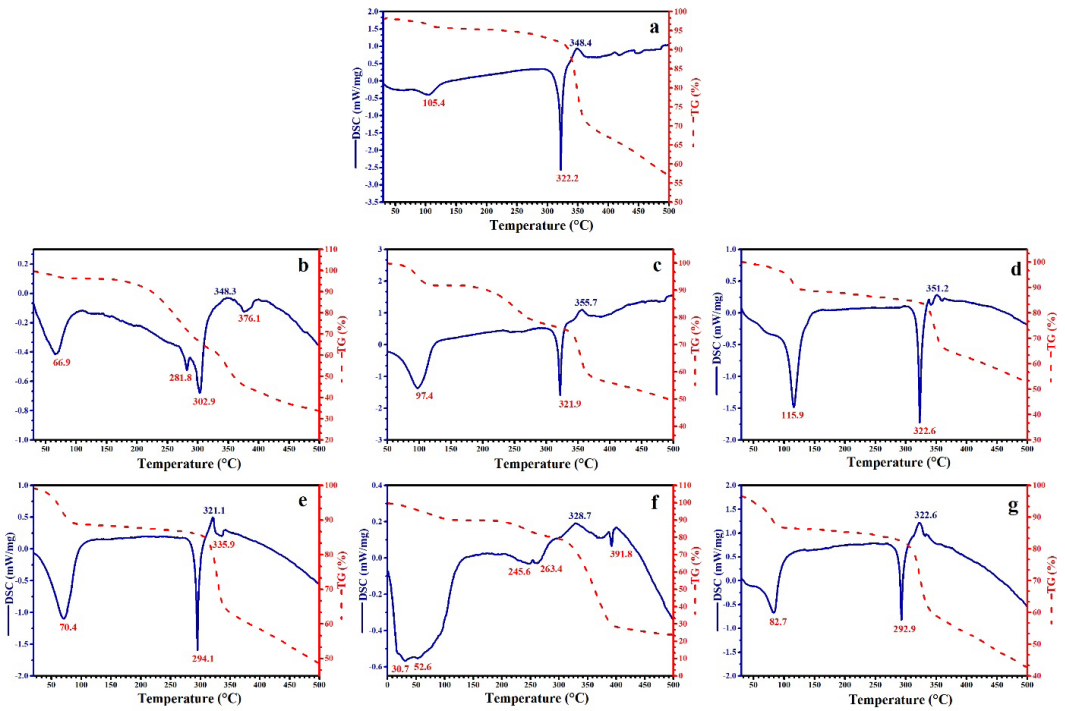

Figure 3. DSC-TG curves of pure QC(a), Group I (drug-oil residues): QC-CO(b), QC-CCO(c), QC-OA(d) and Group II (drug-surfactant residues): QC-T20(e), QC-T60(f) and QC-T80(g).

3.2.2. Non-thermal analysis

3.2.2.1. P-XRD analysis

XRD diffractograms of the pure QC, group I and group II samples have been shown in Figure 4. In our previously published work, we have reported 2Θ (degree) values for major intense peaks of pure QC. The X-ray patterns of pure QC (Fig. 4a) exhibited numerous discrete peaks at 2Θ (degree) values 10.44°, 14.12°, 17.92°, 24.14°, 26.41°, 28.27° and 30.51°, which shows the crystalline nature of the pure drug (QC). Moreover, these results were found to be identical to the reported literature (Dey, Ghosh, Giri, 2020; Kim, 2020; Shi, Fan, Zhang, Sun, He, Li, 2020).

The group I (Fig. 4(b-d)) and group II samples (Fig. 4(e-g)) also showed numerous discrete peaks which ensures that all the samples exhibited crystalline behavior as that of the pure drug. Most of the major peaks in pure QC (Fig. 4a) were retained in group I and group II samples, however the peak intensity at 14.12° (pure QC) was reduced in QC-OA (Fig. 4b), QC-CCO (Fig. 4c) and QC-CO (Fig. 4d). In case of group I and group II samples, intensity of peak in pure QC (11.13°) got increased and shifted slightly to the higher side. Although the intensities of some peaks of the group I and group II samples were reduced, the crystalline nature of the drug was retained in all the samples. Furthermore, the size of the crystallites was estimated using Debye Scherrer's equation, as mentioned above

in the methodology section, and the values have been reported in Table 3. The average particle size ($D_{avg.}$) of the crystalline samples was within the range of 26.80 nm to 76.07 nm. From the results, it was observed that QC-CCO exhibited the lowest $D_{avg.}$ value (26.80 nm) and QC-T20 exhibited the highest $D_{avg.}$ value (76.07). In addition, other analytical studies such as Dynamic Light Scattering (DLS) can be performed to support these findings to detect the effect of these excipients over the particle size and surface charge (zeta potential) of the crude drug.

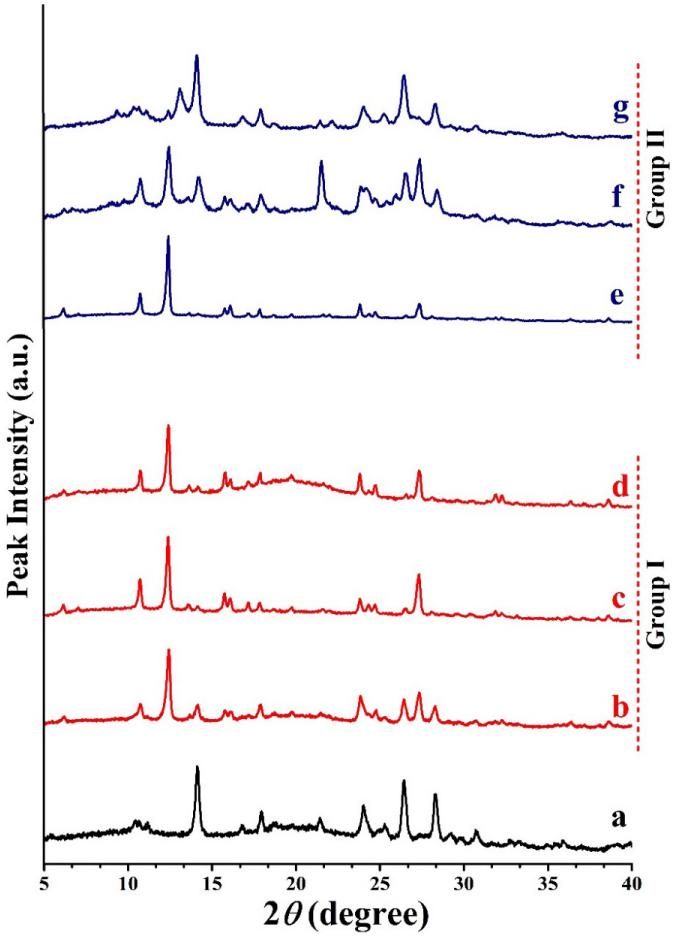

Figure 4. P-XRD diffractograms of pure QC(a), Group I (drug-oil residues): QC-OA(b), QC-CCO(c), QC-CO(d), and Group II (drug-surfactant residues): QC-T20(e), QC-T60(f) and QC-T80(g).

3.2.2.2. FT-IR interpretations

The possible intermolecular interactions between the drug and excipients could be efficiently determined with the help of FT-IR studies (Das, Verma, Singh, 2020b). The FT-IR spectrum of pure QC, Group I and Group II samples have been demonstrated in Figs 5(a), 5(b-d) and 5(e-g) respectively. The FT-IR spectrum of pure QC exhibited characteristic absorption peaks at 3447 cm^{-1} and 3391 cm^{-1} (-OH phenolic stretch), 2925 cm^{-1} and 2853 cm^{-1} (-CH stretch), 1657 cm^{-1} and 1600 cm^{-1} (-C=O stretch), 1513 cm^{-1} and 1432 cm^{-1} (-C=C stretch), 1370 cm^{-1} (-OH phenolic bend), 1326 cm^{-1} (-CH in-plane bending). The multiple peaks between 1265-1015 cm^{-1} were accredited to the –(C-O) and –(C-CO-C) stretch. Furthermore, the absorption bands at 930 cm^{-1}, 826 cm^{-1} and 713 cm^{-1} were accredited to –(CH) out-of-plane bending. Moreover, these results were found to be identical to the reported literature (Catauro, Papale, Bollino, Piccolella, Marciano, Nocera, Pacifico, 2015; Gupta, Kumar, Gupta, Sharma, Verma, Stalin, Chaudhari, Das, Singh, Dwivedi, 2016; Han, Tong, Li, Yu, Hu, Zhang, Xu, Wang, 2021; Lv, Qi, Zou, Zou, Luo, Shao, Tamer, 2019).

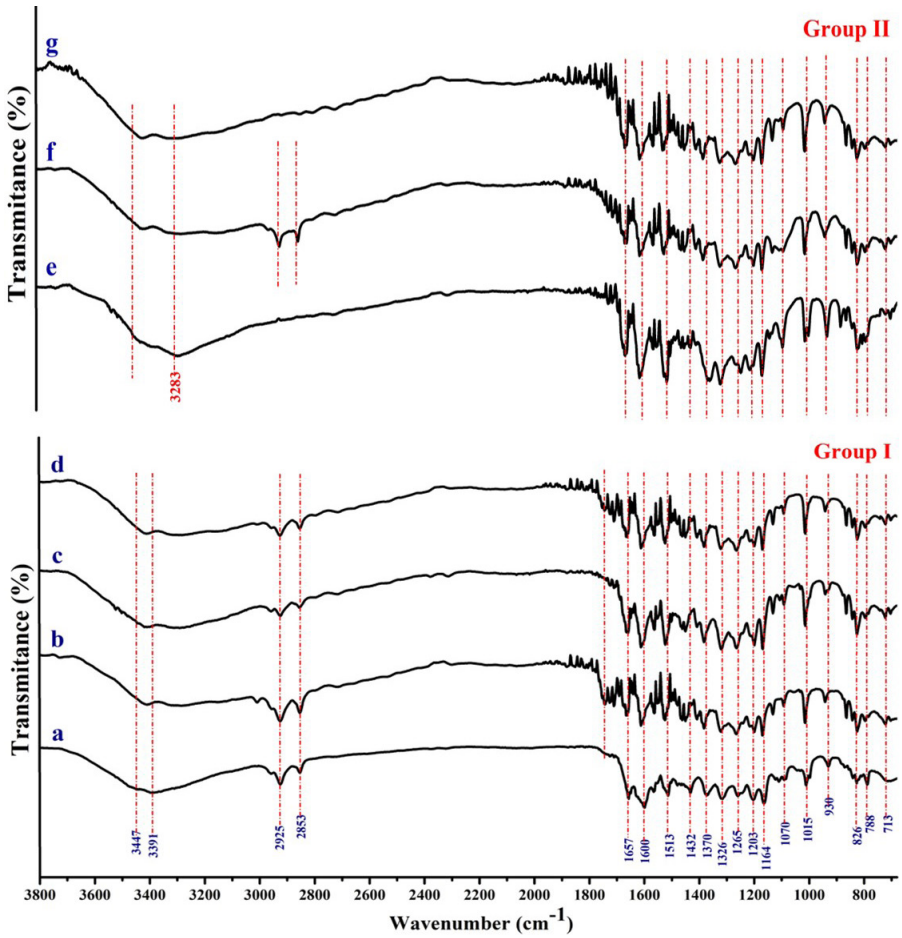

Figure 5. FT-IR spectra of pure QC(a), Group I (drug-oil residues): QC-CO(b), QC-CCO(c), QC-OA(d) and Group II (drug-surfactant residues): QC-T20(e), QC-T60(f) and QC-T80(g).

In QC-CO (Fig. 5b), QC-OA (Fig. 5d), QC-T20 (Fig. 5e), QC-T60 (Fig. 5f) and QC-T80 (Fig. 5g) the band intensity between 1744-1726 cm^{-1} attributed to carbonyl (–C=O) stretching was increased, however, this band was not prominent in pure QC (Fig. 5a) due to very less intensity. Moreover, the band peaks at 2925 cm^{-1} and 2853 cm^{-1} (-CH stretching) of the pure QC was not prominent in QC-T20 (Fig. 5e) and QC-T80 (Fig. 5g). Fig. 5(b-g) demonstrated that the majority of the distinctive peaks of the pure drug (QC) were retained in both Group I and II samples.

Sample Name	2Θ (deg*)	Θ (deg*)	FWHM(β) (deg*)	FWHM(β) (rad#)	rad#	cos (rad#)	$D_{avg.}$ (nm)
Pure QC	14.12	7.06	0.280	0.005	0.123	0.992	28.62
QC-OA	12.4	6.20	0.263	0.005	0.108	0.994	30.39
QC-CCO	12.38	6.19	0.298	0.005	0.108	0.994	26.80
QC-CO	12.4	6.20	0.232	0.004	0.108	0.994	34.49
QC-T20	8.69	4.35	0.105	0.002	0.076	0.997	76.07
QC-T60	8.7	4.35	0.150	0.003	0.076	0.997	53.10
QC-T80	9.54	4.77	0.153	0.003	0.083	0.997	51.95

Table 3. XRD crystallographic data of pure quercetin and quercetin-excipient residues (#rad: radians; *deg: degree).

 https://doi.org/10.37819/nanofab.9.2014

3.2.2.3. Raman spectroscopy interpretations

Raman spectroscopy is widely used for determining the drug-excipient interactions and characterizing the physicochemical properties of pharmaceutical compounds or complex formations. Additionally, as compared to FT-IR or IR spectroscopy, Raman spectroscopy is not obstructed by moisture or water (Das, Verma, Singh, 2020b; Santos, Gerbino, Tymczyszyn, Gomez-Zavaglia, 2015). The Raman spectrum of pure QC, Group I and Group II samples have been demonstrated in Figs 6(a), 6(b-d) and 6(e-g) respectively.

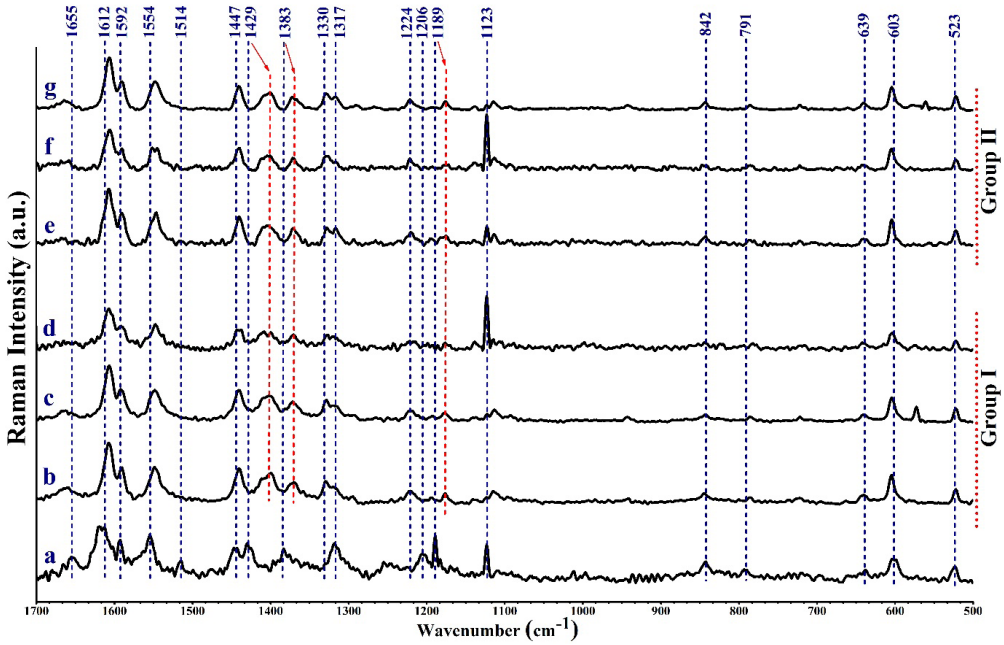

Figure 6. Raman spectra of pure QC(a), Group I (drug-oil residues): QC-CO(b), QC-CCO(c), QC-OA(d) and Group II (drug-surfactant residues): QC-T20(e), QC-T60(f) and QC-T80(g).

The Raman spectrum of pure QC, earlier reported in our work, exhibited the most intense band (doublet) at 1619 cm^{-1} and 1612 cm^{-1} (C2=C3 stretching in ring C and C3/C5-OH in-plane bending). Additionally, pure QC exhibited some other characteristic bands at 1592 cm^{-1} and 1554 cm^{-1} (C=O stretch, ring B -(C-C) stretch; ring A –(C5-OH) stretch), 1447 cm^{-1} (C7-OH bend and C6-C8-H bend), 1429 cm^{-1} (C3/C5-OH bend), 1383 cm^{-1} (ring A -(C3/C5/C7-OH) bend), 1317 cm^{-1} (ring C –(C3-OH) bend or ring B –(C3′-OH) bend), 1189 cm^{-1} (C3′-O bend), 1123 cm^{-1} (C3-OH, C3′/C4′-OH and C-C-H bend), 842 cm^{-1} (C-C and C-H stretch), 603 cm^{-1} and 523 cm^{-1} (ring B-C stretch). Also, some less intense bands were noticed at 1655 cm^{-1} (C4=O stretch), 1514 cm^{-1} (ring A –(C-C) stretch), 1330 cm^{-1} (ring C –(C3-OH) bend), 1224 cm^{-1} and 1206 cm^{-1} (ring B –(C4′-OH) bend). These findings were found to be similar to the earlier reported works (Das, Verma, Singh, 2020b; Qiao, Cao, Yu, Zong, Pu, 2020; Shi, Fan, Zhang, Sun, He, Li, 2020).

Although most of the bands of pure QC (Fig. 6a) were retained in both Group I and II samples (Fig. 6b-g), some irregularities in bands were observed. The bands of pure QC at 1429 cm^{-1}, 1383 cm^{-1} and 1189 cm^{-1} corresponding to C3/C5-OH bend, ring A –(C3/C5/C7-OH) bend and C3′-O bend, respectively were shifted to lower frequencies in all other samples (represented through red dotted lines in Fig. 6). Also, the band intensity of pure QC at 1330 cm^{-1} (ring C –(C3-OH) bend) was increased in all samples. However, the band intensity of pure QC at 1514 cm^{-1} (ring A –(C-C) stretch) was decreased in all samples and even disappeared in QC-T80 (Fig. 6i). The occurrence of band shifting and alterations in band intensities could be due to intermolecular hydrogen bonding (C7-OH) or interactions of excipients with the hydroxy groups (-OH) present in QC molecule (Baranovic Segota, 2018; Borghetti, Lula, Sinisterra, Bassani, 2009; Dimitric Markovic, Markovic, Milenkovic, Jeremic, 2011; Zdyb Krawczyk, 2016).

3.2.2.4. Morphological Analysis: FESEM

FESEM technique is highly applicable for visualizing very small (in the nanometer range) topographic particulars over the surface or whole or fraction of samples. The FESEM micrograph of pure QC (Fig.7a) exhibited a systematic rough crystal habit with a long cylindrical flake appearance. Similar findings for pure QC were reported in earlier literature (Das, Verma, Singh, 2020b; Han, Tong, Li, Yu, Hu, Zhang, Xu, Wang, 2021; Kakran, Shegokar, Sahoo, Shaal, Li, Muller, 2012; Li Y., Gao, Ji, Liu, Liu, Yang, Lu, Han, Wang, 2020). The FESEM microstructures of pure QC, Group I and Group II samples have been represented in Fig. 7(a), 7(b-d) and 7(e-g) respectively.

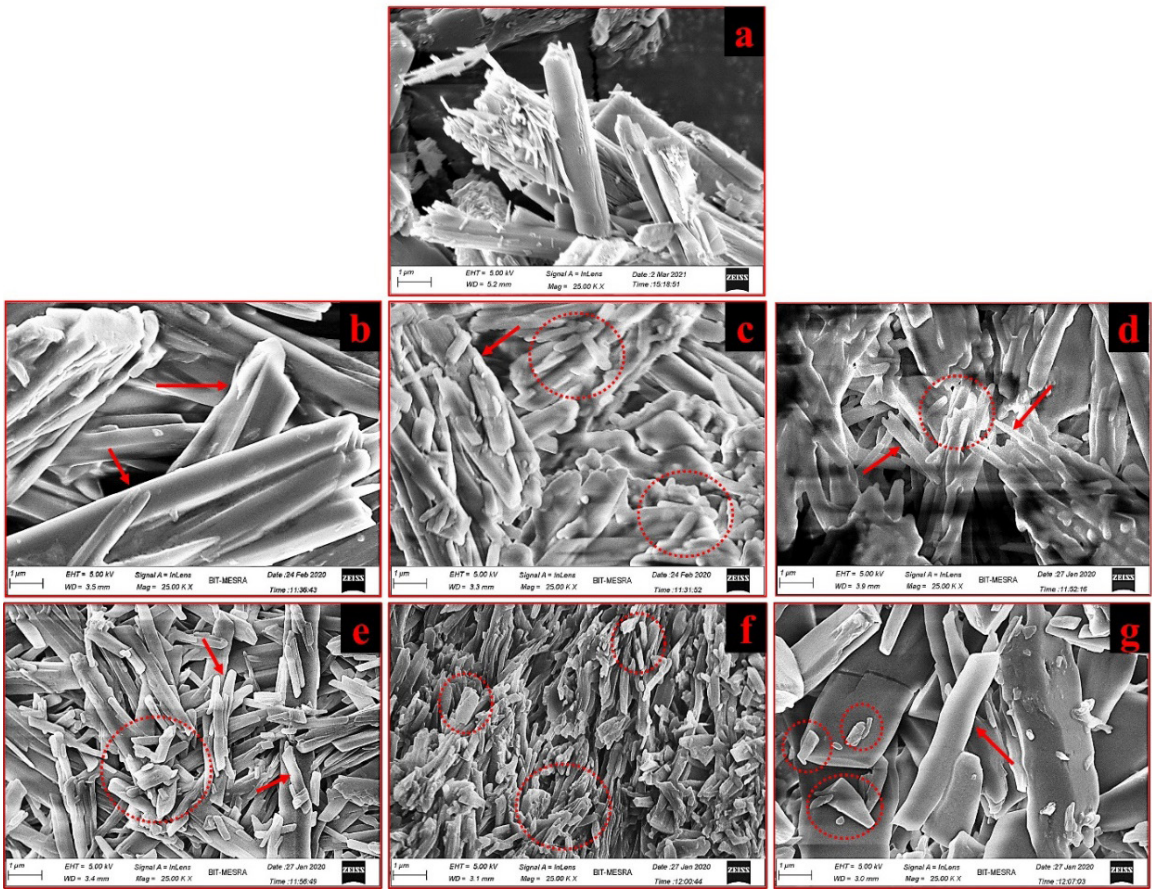

Figure 7. FESEM micrographs of pure QC(a), Group I (drug-oil residues): QC-CO(b), QC-CCO(c), QC-OA(d) and Group II (drug-surfactant residues): QC-T20(e), QC-T60(f) and QC-T80(g).

In group I samples, the micrograph of QT-CO (Fig. 7b) exhibited similar patterns to pure QC, though the surface of crystals was smoothed (red arrows). In the case of QT-CCO (Fig. 7c) and QT-OA (Fig. 7d), the surface of drug crystals was smoothed (red arrows) and agglomerated, also the particles were found to be in a dissolved state (red dotted circles). In group II samples, the micrographs of QC-T20 (Fig. 7e), QC-T60 (Fig. 7f) and QC-T80 (Fig. 7g) exhibited a similar crystal pattern as that of a pure drug (Fig. 7a). Moreover, the surface of crystals was smoothed (red arrows) and also fragmentation of particles (red dotted circles) was noticed in all the three samples. However, in the case of QC-T60 high level of crystal fragmentation was observed as compared QC-T20 and QC-T60. Overall, all the samples exhibited similar crystal habits as that of pure QC but surface smoothening, agglomeration and fragmentation were observed in samples. This shows that the presence of excipient might impart a significant impact over the crystal lattice of pure drug and thus affect the solubility and bioavailability of QC.

4. CONCLUSIONS

In this work, the compatibility and stability of pure quercetin with various food-grade excipients (CCO, CO, OA, T20, T60 and T80) were studied through thermal (DSC and TGA), non-thermal (P-XRD, FT-IR and Raman spectroscopy, and FESEM) methods of analysis. All the methods were found to be effective and reliable for performing the compatibility studies of pure QC and QC-excipient residues. DSC-TG studies showed that as compared to other excipients, CO and T60 exhibited irregular degradation patterns and thus extremely affected the properties of the drug leading to transformations from crystalline to amorphous nature. P-XRD results showed that the peak intensities of some samples were reduced and shifted but the crystalline behavior of QC was retained in all the samples. Also, the values of $D_{avg.}$ of the crystalline samples were found to be in the range of 16.85-76.07 nm, using Debye Scherrer's equation. FTIR interpretations showed that major of the peaks (fingerprint regions) were retained in all the samples, however, the band intensity between 1744-1726 cm^{-1} was increased in almost all samples, probably due to –C=O stretching. RAMAN interpretations showed that the band intensity of pure QC at 1330 cm^{-1} (ring C –(C3-OH) bend) was increased in all samples. However, the band intensity of pure QC at 1514 cm^{-1} (C-C stretching of ring A) was decreased in all samples and even disappeared in QC-T80. These results conclude that –C=O stretch, ring A –(C-C) and -OH bonds can play a significant role in maintaining the stability of QC. Additionally, the FESEM micrographs concluded that the presence of excipients might show significant influence over the crystal lattice of QC, thus influencing its solubility and bioavailability.

These studies are found to be important and play a vital role in product development because phase transitions resulting from drug-excipient interactions might cause significant alterations in the physicochemical properties of the drug. Moreover, these physicochemical properties can act as an important source for researchers and manufacturers to accomplish in-process control in the development of pharmaceutical, cosmeceutical and nutraceutical products.

Authors Contributions

S.S.D. executed and drafted the experimentations. P.R.P.V performed data curation in the manuscript. The whole research work was accomplished under the supervision of S. K. S.

Conflict of interest

All the authors have read the manuscript carefully and declare no conflict of interest. ♦

REFERENCES

Agrawal K, Chakraborty P, Dewanjee S, Arfin S, Das SS, Dey A, Moustafa M, Mishra PC, Jafari SM, Jha NK, Jha SK, Kumar D (2023) Neuropharmacological interventions of quercetin and its derivatives in neurological and psychological disorders. Neurosci Biobehav Rev 144: 104955. doi:10.1016/j.neubiorev.2022.104955.

Alkhatib MH, Alyamani SA, Abdu F (2020) Incorporation of methotrexate into coconut oil nanoemulsion potentiates its antiproliferation activity and attenuates its oxidative stress. Drug Deliv 27: 422-430. doi:10.1080/10717544.2020.1736209.

Anarjan N, Tan CP (2013) Effects of selected polysorbate and sucrose ester emulsifiers on the physicochemical properties of astaxanthin nanodispersions. Molecules 18: 768-777. doi:10.3390/molecules18010768.

Balestrin LA, Bidone J, Bortolin RC, Moresco K, Moreira JC, Teixeira HF (2016) Protective effect of a hydrogel containing Achyrocline satureioides extract-loaded nanoemulsion against UV-induced skin damage. J Photochem Photobiol B 163: 269-276. doi:10.1016/j.jphotobiol.2016.08.039.

Baranovic G, Segota S (2018) Infrared spectroscopy of flavones and flavonols. Reexamination of the hydroxyl and carbonyl vibrations in relation to the interactions of flavonoids with membrane lipids. Spectrochim Acta A Mol Biomol Spectrosc 192: 473-486. doi:10.1016/j.saa.2017.11.057.

Barkat Ali K (2011) Basics of pharmaceutical emulsions: A review. African Journal of Pharmacy and Pharmacology 5. doi:10.5897/ajpp11.698.

Basiri L, Rajabzadeh G, Bostan A (2017) Physicochemical properties and release behavior of Span 60/Tween 60 niosomes as vehicle for α-Tocopherol delivery. Lwt 84: 471-478. doi:10.1016/j.lwt.2017.06.009.

Bischoff SC (2008) Quercetin: potentials in the prevention and therapy of disease. Curr Opin Clin Nutr Metab Care 11: 733-740. doi:10.1097/MCO.0b013e32831394b8.

Borghetti GS, Lula IS, Sinisterra RD, Bassani VL (2009) Quercetin/beta-cyclodextrin solid complexes prepared in aqueous solution followed by spray-drying or by physical mixture. AAPS PharmSciTech 10: 235-242. doi:10.1208/s12249-009-9196-3.

Bruni G, Amici L, Berbenni V, Marini A, Orlandi A (2002) Drug-Excipient Compatibility Studies. Search of interaction indicators. Journal of Thermal Analysis and Calorimetry 68: 561-573. doi:10.1023/a:1016052121973.

Catauro M, Papale F, Bollino F, Piccolella S, Marciano S, Nocera P, Pacifico S (2015) Silica/quercetin sol-gel hybrids as antioxidant dental implant materials. Sci Technol Adv Mater 16: 035001. doi:10.1088/1468-6996/16/3/035001.

Chassaing B, Koren O, Goodrich JK, Poole AC, Srinivasan S, Ley RE, Gewirtz AT (2015) Dietary emulsifiers impact the mouse gut microbiota promoting colitis and metabolic syndrome. Nature 519: 92-96. doi:10.1038/nature14232.

Crowley P, Martini L (2001) Drug-Excipient Interactions. Pharmaceutical Technology Europe 13: 26-31.

D'Andrea G (2015) Quercetin: A flavonol with multifaceted therapeutic applications? Fitoterapia 106: 256-271. doi:10.1016/j.fitote.2015.09.018.

Das SS, Dubey AK, Verma PRP, Singh SK, Singh SK (2022) Therapeutic Potential of Quercetin-Loaded Nanoemulsion against Experimental Visceral Leishmaniasis: In Vitro/Ex Vivo Studies and Mechanistic Insights. Mol Pharm 19: 3367-3384. doi:10.1021/acs.molpharmaceut.2c00492.

Das SS, Hussain A, Verma PRP, Imam SS, Altamimi MA, Alshehri S, Singh SK (2020) Recent Advances in Liposomal Drug Delivery System of Quercetin for Cancer Targeting: A Mechanistic Approach. Curr Drug Deliv 17: 845-860. doi:10.2174/1567201817666200415112657.

Das SS, Jha NK, Jha SK, Verma PRP, Ashraf GM, Singh SK (2023) Neuroprotective Role of Quercetin against Alpha-Synuclein-Associated Hallmarks in Parkinson's Disease. Curr Neuropharmacol 21: 1464-1466. doi:10.2174/1570159X21666221221092250.

Das SS, Sarkar A, Chabattula SC, Verma PRP, Nazir A, Gupta PK, Ruokolainen J, Kesari KK, Singh SK (2022) Food-Grade Quercetin-Loaded Nanoemulsion Ameliorates Effects Associated with Parkinson's Disease and Cancer: Studies Employing a Transgenic C. elegans Model and Human Cancer Cell Lines. Antioxidants (Basel) 11. doi:10.3390/antiox11071378.

Das SS, Verma PRP, Kar S, Singh SK (2020). Quercetin-Loaded Nanomedicine as Oncotherapy. In Nanomedicine for Bioactives (pp. 155-183).

Das SS, Verma PRP, Sekarbabu V, Mohanty S, Pattnaik AK, Ruokolainen J, Kesari KK, Singh SK (2023) Liquid Chromatography-Electrospray Ionization Tandem Mass Spectrometry Estimation of Quercetin-Loaded Nanoemulsion in Rabbit Plasma: In Vivo-In Silico Pharmacokinetic Analysis Using GastroPlus. ACS Omega 8: 12456-12466. doi:10.1021/acsomega.3c00429.

Das SS, Verma PRP, Singh SK (2020a). Quercetin-Loaded Nanomedicine as Nutritional Application. In Nanomedicine for Bioactives (pp. 259-301).

Das SS, Verma PRP, Singh SK (2020b) Screening and preparation of quercetin doped nanoemulsion: characterizations, antioxidant and anti-bacterial activities. LWT-Food Sci Technol 124. doi:10.1016/j.lwt.2020.109141.

Dey M, Ghosh B, Giri TK (2020) Enhanced intestinal stability and pH sensitive release of quercetin in GIT through gellan gum hydrogels. Colloids Surf B Biointerfaces 196: 111341. doi:10.1016/j.colsurfb.2020.111341.

Dimitric Markovic JM, Markovic ZS, Milenkovic D, Jeremic S (2011) Application of comparative vibrational spectroscopic and mechanistic studies in analysis of fisetin structure. Spectrochim Acta A Mol Biomol Spectrosc 83: 120-129. doi:10.1016/j.saa.2011.08.001.

Dinesh Kumar V, Verma PRP, Singh SK (2015) Development and evaluation of biodegradable polymeric nanoparticles for the effective delivery of quercetin using a quality by design approach. LWT-Food Sci Technol 61: 330-338. doi:10.1016/j.lwt.2014.12.020.

Dupont J, White PJ, Carpenter MP, Schaefer EJ, Meydani SN, Elson CE, Woods M, Gorbach SL (1990) Food uses and health effects of corn oil. J Am Coll Nutr 9: 438-470. doi:10.1080/07315724.1990.10720403.

Fuentes J, Arias-Sante MF, Atala E, Pastene E, Kogan MJ, Speisky H (2020) Low nanomolar concentrations of a quercetin oxidation product, which naturally occurs in onion peel, protect cells against oxidative damage. Food Chem 314: 126166. doi:10.1016/j.foodchem.2020.126166.

Gallelli G, Cione E, Serra R, Leo A, Citraro R, Matricardi P, Di Meo C, Bisceglia F, Caroleo

MC, Basile S, Gallelli L (2020) Nano-hydrogel embedded with quercetin and oleic acid as a new formulation in the treatment of diabetic foot ulcer: A pilot study. Int Wound J 17: 485-490. doi:10.1111/iwj.13299.

Gao X, Wang B, Wei X, Men K, Zheng F, Zhou Y, Zheng Y, Gou M, Huang M, Guo G, Huang N, Qian Z, Wei Y (2012) Anticancer effect and mechanism of polymer micelle-encapsulated quercetin on ovarian cancer. Nanoscale 4: 7021-7030. doi:10.1039/c2nr32181e.

Garcia-Mendoza MDP, Espinosa-Pardo FA, Savoire R, Harscoat-Schiavo C, Cansell M, Subra-Paternault P (2021) Improvement of the oxidative stability of camelina oil by enrichment with phospholipid-quercetin formulations. Food Chem 341: 128234. doi:10.1016/j.foodchem.2020.128234.

German JB (1999) Food processing and lipid oxidation. Adv Exp Med Biol 459: 23-50. doi:10.1007/978-1-4615-4853-9_3.

Gupta K, Kumar S, Gupta RK, Sharma A, Verma AK, Stalin K, Chaudhari BP, Das M, Singh SP, Dwivedi PD (2016) Reversion of Asthmatic Complications and Mast Cell Signalling Pathways in BALB/c Mice Model Using Quercetin Nanocrystals. J Biomed Nanotechnol 12: 717-731. doi:10.1166/jbn.2016.2197.

Han J, Tong M, Li S, Yu X, Hu Z, Zhang Q, Xu R, Wang J (2021) Surfactant-free amorphous solid dispersion with high dissolution for bioavailability enhancement of hydrophobic drugs: a case of quercetin. Drug Dev Ind Pharm 47: 153-162. doi:10.1080/03639045.2020.1862173.

Hemati M, Haghiralsadat F, Yazdian F, Jafari F, Moradi A, Malekpour-Dehkordi Z (2019) Development and characterization of a novel cationic PEGylated niosome-encapsulated forms of doxorubicin, quercetin and siRNA for the treatment of cancer by using combination therapy. Artif Cells Nanomed Biotechnol 47: 1295-1311. doi:10.1080/21691401.2018.1489271.

Kakran M, Shegokar R, Sahoo NG, Shaal LA, Li L, Muller RH (2012) Fabrication of quercetin nanocrystals: comparison of different methods. Eur J Pharm Biopharm 80: 113-121. doi:10.1016/j.ejpb.2011.08.006.

Kamoun O, Gassoumi A, Kouass S, Alhalaili B, Vidu R, Turki-Kamoun N (2020) An Investigation on the Synthesis of Molybdenum Oxide and Its Silica Nanoparticle Composites for Dye Degradation. Nanomaterials (Basel) 10. doi:10.3390/nano10122409.

Kar S, Das SS, Kundu S, Sahu BD, Kumar KJ, Kesari KK, Singh SK (2024) Intranasal Delivery of Carvedilol- and Quercetin-Encapsulated Cationic Nanoliposomes for Cardiovascular Targeting: Formulation and In Vitro and Ex Vivo Studies. ACS Appl Bio Mater. doi:10.1021/acsabm.4c00102.

Kar S, Das SS, Singh SK (2023) Quercetin-encapsulated magnetoliposomes: Fabrication, optimization, characterization, and antioxidant studies. European Journal of Lipid Science and Technology 125. doi:10.1002/ejlt.202300112.

Khalid N, Kobayashi I, Neves MA, Uemura K, Nakajima M, Nabetani H (2016) Microchannel emulsification study on formulation and stability characterization of monodisperse oil-in-water emulsions encapsulating quercetin. Food Chem 212: 27-34. doi:10.1016/j.foodchem.2016.05.154.

Kim JS (2020) Study of Flavonoid/Hydroxypropyl-beta-Cyclodextrin Inclusion Complexes by UV-Vis, FT-IR, DSC, and X-Ray Diffraction Analysis. Prev Nutr Food Sci 25: 449-456. doi:10.3746/pnf.2020.25.4.449.

Kiokias S, Gordon MH, Oreopoulou V (2017) Effects of composition and processing variables on the oxidative stability of protein-based and oil-in-water food emulsions. Crit Rev Food Sci Nutr 57: 549-558. doi:10.1080/10408398.2014.893503.

Li S, Yan Y, Guan X, Huang K (2020) Preparation of a hordein-quercetin-chitosan antioxidant electrospun nanofibre film for food packaging and improvement of the film hydrophobic properties by heat treatment. Food Packaging and Shelf Life 23. doi:10.1016/j.fpsl.2020.100466.

Li Y, Gao S, Ji X, Liu H, Liu N, Yang J, Lu M, Han L, Wang M (2020) Evaluation studies on effects of quercetin with different concentrations on the physicochemical properties and in vitro digestibility of Tartary buckwheat starch. Int J Biol Macromol 163: 1729-1737. doi:10.1016/j.ijbiomac.2020.09.116.

Lillard DA (1983) Effect of Processing on Chemical and Nutritional Changes in Food Lipids. J Food Prot 46: 61-67. doi:10.4315/0362-028X-46.1.61.

Liu D, Hu H, Lin Z, Chen D, Zhu Y, Hou S, Shi X (2013) Quercetin deformable liposome: preparation and efficacy against ultraviolet B induced skin damages in vitro and in vivo. J Photochem Photobiol B 127: 8-17. doi:10.1016/j.jphotobiol.2013.07.014.

Liu D, Kobayashi T, Russo S, Li F, Plevy SE, Gambling TM, Carson JL, Mumper RJ (2013) In vitro and in vivo evaluation of a water-in-oil microemulsion system for enhanced peptide intestinal delivery. AAPS J 15: 288-298. doi:10.1208/s12248-012-9441-7.

Lv R, Qi L, Zou Y, Zou J, Luo Z, Shao P, Tamer TM (2019) Preparation and structural properties of amylose complexes with quercetin and their preliminary evaluation in delivery application. International Journal of Food Properties 22: 1445-1462. doi:10.1080/10942912.2019.1651736.

Makris DP, Rossiter JT (2000) Heat-induced, metal-catalyzed oxidative degradation of quercetin and rutin (Quercetin 3-O-rhamnosylglucoside) in aqueous model systems. J Agric Food Chem 48: 3830-3838. doi:10.1021/jf0001280.

Manta K, Papakyriakopoulou P, Chountoulesi M, Diamantis DA, Spaneas D, Vakali V, Naziris N, Chatziathanasiadou MV, Andreadelis I, Moschovou K, Athanasiadou I, Dallas P, Rekkas DM, Demetzos C, Colombo G, Banella S, Javornik U, Plavec J, Mavromoustakos T, Tzakos AG, Valsami G (2020) Preparation and Biophysical Characterization of Quercetin Inclusion Complexes with beta-Cyclodextrin Derivatives to be Formulated as Possible Nose-to-Brain Quercetin Delivery Systems. Mol Pharm 17: 4241-4255. doi:10.1021/acs.molpharmaceut.0c00672.

Olejniczak S, Potrzebowski MJ (2004) Solid state NMR studies and density functional theory (DFT) calculations of conformers of quercetin. Org Biomol Chem 2: 2315-2322. doi:10.1039/b406861k.

Qiao Y, Cao Y, Yu K, Zong L, Pu X (2020) Preparation and antitumor evaluation of quercetin nanosuspensions with synergistic efficacy and regulating immunity. Int J Pharm 589: 119830. doi:10.1016/j.ijpharm.2020.119830.

Ramachandran S, Dash CS, Thamilselvan A, Kalpana S, Sundararajan M (2020) Rapid Synthesis and Characterization of Pure and Cobalt Doped Zinc Aluminate Nanoparticles via Microwave Assisted Combustion Method. J Nanosci Nanotechnol 20: 2382-2388. doi:10.1166/jnn.2020.17314.

Sales-Campos H, Reis de Souza P, Crema Peghini B, Santana da Silva J, Ribeiro Cardoso C (2013) An Overview of the Modulatory Effects of Oleic Acid in Health and Disease. Mini-Reviews in Medicinal Chemistry 13: 201-210. doi:10.2174/1389557511313020003.

Santos MI, Gerbino E, Tymczyszyn E, Gomez-Zavaglia A (2015) Applications of Infrared and Raman Spectroscopies to Probiotic Investigation. Foods 4: 283-305. doi:10.3390/foods4030283.

Schoener AL, Zhang R, Lv S, Weiss J, McClements DJ (2019) Fabrication of plant-based vitamin D3-fortified nanoemulsions: influence of carrier oil type on vitamin bioaccessibility. Food Funct 10: 1826-1835. doi:10.1039/c9fo00116f.

Sedaghat Doost A, Kassozi V, Grootaert C, Claeys M, Dewettinck K, Van Camp J, Van der Meeren P (2019) Self-assembly, functionality, and in-vitro properties of quercetin loaded nanoparticles based on shellac-almond gum biological macromolecules. Int J Biol Macromol 129: 1024-1033. doi:10.1016/j.ijbiomac.2019.02.071.

Seneviratne KN, HapuarachchI CD, Ekanayake S (2009) Comparison of the phenolic-dependent antioxidant properties of coconut oil extracted under cold and hot conditions. Food Chemistry 114: 1444-1449. doi:10.1016/j.foodchem.2008.11.038.

Shi X, Fan N, Zhang G, Sun J, He Z, Li J (2020) Quercetin amorphous solid dispersions prepared by hot melt extrusion with enhanced solubility and intestinal absorption. Pharm Dev Technol 25: 472-481. doi:10.1080/10837450.2019.1709502.

Singh N, Hussain A, Kumar Singh S (2020) Morphological transitions of Bacillus subtilis in the presence of food-grade lipidic nanoemulsions. J Food Sci 85: 1223-1230. doi:10.1111/1750-3841.15088.

Teo A, Goh KK, Wen J, Oey I, Ko S, Kwak HS, Lee SJ (2016) Physicochemical properties of whey protein, lactoferrin and Tween 20 stabilised nanoemulsions: Effect of temperature, pH and salt. Food Chem 197: 297-306. doi:10.1016/j.foodchem.2015.10.086.

Thumma S, Repka MA (2009) Compatibility studies of promethazine hydrochloride with tablet excipients by means of thermal and non-thermal methods. Pharmazie 64: 183-189. doi:10.1691/ph.2009.8268.

Tuncer M, Bakan F, Gocmez H, Erdem E (2019) Capacitive behaviour of nanocrystalline octacalcium phosphate (OCP) (Ca8H2(PO4)6.5H2O) as an electrode material for supercapacitors: biosupercaps. Nanoscale 11: 18375-18381. doi:10.1039/c9nr07108c.

Vaz GR, Clementino A, Bidone J, Villetti MA, Falkembach M, Batista M, Barros P, Sonvico F, Dora C (2020) Curcumin and Quercetin-Loaded

Nanoemulsions: Physicochemical Compatibility Study and Validation of a Simultaneous Quantification Method. Nanomaterials (Basel) 10. doi:10.3390/nano10091650.

Verma RK, Garg S (2005) Selection of excipients for extended release formulations of glipizide through drug-excipient compatibility testing. J Pharm Biomed Anal 38: 633-644. doi:10.1016/j.jpba.2005.02.026.

Wang Z, Zou W, Liu L, Wang M, Li F, Shen W (2021) Characterization and bacteriostatic effects of beta-cyclodextrin/quercetin inclusion compound nanofilms prepared by electrospinning. Food Chem 338: 127980. doi:10.1016/j.foodchem.2020.127980.

Wyttenbach N, Birringer C, Alsenz J, Kuentz M (2005) Drug-excipient compatibility testing using a high-throughput approach and statistical design. Pharm Dev Technol 10: 499-505. doi:10.1080/10837450500299875.

Zdyb A, Krawczyk S (2016) Characterization of adsorption and electronic excited states of quercetin on titanium dioxide nanoparticles. Spectrochim Acta A Mol Biomol Spectrosc 157: 197-203. doi:10.1016/j.saa.2016.01.006.

Zhang GG, Law D, Schmitt EA, Qiu Y (2004) Phase transformation considerations during process development and manufacture of solid oral dosage forms. Adv Drug Deliv Rev 56: 371-390. doi:10.1016/j.addr.2003.10.009.